International Journal of
Molecular Sciences

MDPI

Article

The Discovery of Novel α_{2a} Adrenergic Receptor Agonists Only Coupling to Gαi/O Proteins by Virtual Screening

Peilan Zhou *, Fengfeng Lu, Huili Zhu, Beibei Shi, Xiaoxuan Wang, Shiyang Sun, Yulei Li and Ruibin Su *

State Key Laboratory of Toxicology and Medical Countermeasures, Beijing Key Laboratory of Neuropsychopharmacology, Beijing Institute of Pharmacology and Toxicology, 27th Taiping Road, Beijing 100850, China; lff8591465@163.com (F.L.); a123zhuzhujy@163.com (H.Z.); shigogogo123@163.com (B.S.); sepchutz0807@163.com (X.W.); noah97sun@163.com (S.S.); bettylpaine@163.com (Y.L.)

* Correspondence: zhoupl@bmi.ac.cn (P.Z.); surb@bmi.ac.cn (R.S.); Tel.: +86-10-66931624 (P.Z.); +86-10-66931601 (R.S.)

Abstract: Most α_2-AR agonists derived from dexmedetomidine have few structural differences between them and have no selectivity for $\alpha_{2A/2B}$-AR or Gi/Gs, which can lead to side effects in drugs. To obtain novel and potent α_{2A}-AR agonists, we performed virtual screening for human α_{2A}-AR and α_{2B}-AR to find α_{2A}-AR agonists with higher selectivity. Compound P300–2342 and its three analogs significantly decreased the locomotor activity of mice ($p < 0.05$). Furthermore, P300–2342 and its three analogs inhibited the binding of [^{3}H] Rauwolscine with IC_{50} values of 7.72 ± 0.76 and 12.23 ± 0.11 μM, respectively, to α_{2A}-AR and α_{2B}-AR. In α_{2A}-AR-HEK293 cells, P300–2342 decreased forskolin-stimulated cAMP production without increasing cAMP production, which indicated that P300–2342 activated α_{2A}-AR with coupling to the Gαi/o pathway but without Gαs coupling. P300–2342 exhibited no agonist but slight antagonist activities in α_{2B}-AR. Similar results were obtained for the analogs of P300–2342. The docking results showed that P300–2342 formed π-hydrogen bonds with Y394, V114 in α_{2A}-AR, and V93 in α_{2B}-AR. Three analogs of P300–2342 formed several π-hydrogen bonds with V114, Y196, F390 in α_{2A}-AR, and V93 in α_{2B}-AR. We believe that these molecules can serve as leads for the further optimization of α_{2A}-AR agonists with potentially few side effects.

Keywords: α_{2A} adrenergic receptor; virtual screening; Gαi/o proteins

check for updates

Citation: Zhou, P.; Lu, F.; Zhu, H.; Shi, B.; Wang, X.; Sun, S.; Li, Y.; Su, R. The Discovery of Novel α_{2a} Adrenergic Receptor Agonists Only Coupling to Gαi/O Proteins by Virtual Screening. *Int. J. Mol. Sci.* **2024**, *25*, 7233. https://doi.org/10.3390/ijms25137233

Academic Editor: Ralf Herwig

Received: 26 April 2024
Revised: 23 June 2024
Accepted: 26 June 2024
Published: 30 June 2024

Copyright: © 2024 by the authors. Licensee MDPI, Basel, Switzerland. This article is an open access article distributed under the terms and conditions of the Creative Commons Attribution (CC BY) license (https://creativecommons.org/licenses/by/4.0/).

1. Introduction

Alpha2-adrenergic receptors (α_2-AR) are integral membrane proteins that belong to the superfamily of G-protein-coupled receptors (GPCRs). These receptors regulate effector function via activation of multiple members of Go and Gi G-protein families [1]. Three subtypes (α2A/α2-C10, α2B/α2-C2, and α2C/α2-C4) are encoded by distinct genes and widely expressed in the brain. α_{2A}-AR is most abundant in the rat locus coeruleus, but is also widely localized in the brain stem, cerebral cortex, septum, hypothalamus, hippocampus, and amygdala. α_{2B}-AR was observed only in the thalamus, while α_{2C}-AR was mainly distributed in the basal ganglia, olfactory tubercle, hippocampus, and cerebral cortex [2]. α_{2A}-AR is the predominant α_2-AR subtype in the central nervous system, which prejunctionally inhibits the release of sympathetic, endogenous neurotransmitters such as norepinephrine and epinephrine. They mediate the antihypertensive and the sedative effects of α_2-AR agonists [3,4]. The postjunctional α_2-AR found in the peripheral tissues has been demonstrated to induce vasoconstriction and increase arterial pressure in various mammalian species [5,6]. The α_{2B}-AR subtype is mainly distributed in the periphery, including lung, kidney, liver, heart, and vascular tissues. It appears to have a dominant role in eliciting the immediate or salt-loading hypertensive response to α_2-AR agonists [7–9]. α_{2C}-AR regulates the release of norepinephrine at low norepinephrine concentrations, in contrast to α_{2A}-AR regulation at high norepinephrine concentrations [3]. The amount of

α_{2C}-AR is lower than that of α_{2A}-AR in the brain. The autoinhibition mediated by α_{2C}-AR in α_{2C}-KO mice could be substituted by α_{2A}-AR for the elusive character of α_{2C}-AR [10].

A large amount of structural activity data has emerged in pursuit of the specific agonists and antagonists of α_2-AR subtypes for potential therapeutics since the discovery of the three α_2-AR subtypes. Exceptionally, α_{2A}-AR has a dual pharmacological effect in that it simultaneously couples to Gi and Gs to inhibit or stimulate adenylyl cyclase (AC) activity [11]. At low agonist concentrations, α_{2A}-AR mainly couples to Gi, whereas at high concentrations, Gs coupling dominates. This unusual dual effect has not been well understood for any GPCR. The Gi/o inhibitor pertussis toxin (PTX) pre-treatment inhibited DMED-induced sedation [12], whereas the Gs inhibitor had no effect on the sedation induced by DMED (data not published). The Gs coupling action of these partial agonists of α_{2A}-AR may not be related to sedation, and the effects remain incompletely understood. α_{2A}-AR agonists are mainly imidazole ring compounds that can interact with D113 by a salt bridge, and they have no selectivity for $\alpha_{2A/2B}$-AR or Gi/Gs [13]. To enhance the therapeutic potency of α_2 agonists as antihypertensive and sedative drugs, compounds should bind to α_{2B}-AR with lower affinity or have no coupling to Gs proteins at high concentrations.

Computer-aided drug design has been widely used to discover novel and potent lead compounds. This study combined crystal structures for human α_{2A}-AR [14] and α_{2B}-AR [15] with virtual screening to obtain highly selective α_{2A}-AR agonists as potential sedatives. The ChemDiv compound library (1,535,478 compounds) was screened, and 1023 compounds were found that could bind to α_{2A}-AR with high affinity but low affinity to α_{2B}-AR. We selected 105 compounds with good druggability according to the virtual screening; these molecules were studied in the loss of righting reflex (LORR) of C57/B6 mice. Compound P300–2342 and three analogs had a sedative effect after α_{2A}-AR activation, as did the Gi/o-coupled pathway with the inhibition of AC-cyclic adenosine monophosphate (cAMP) accumulation. These compounds could serve as leads for sedation by α_{2A}-AR activation with potentially few side effects.

2. Results

2.1. Analysis of the Molecular Docking Results

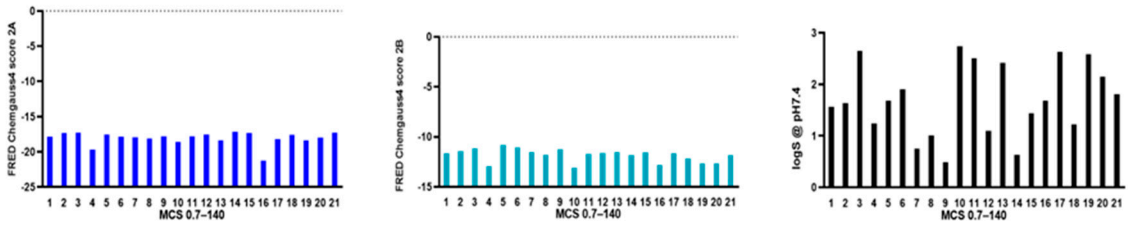
All 50,679,311 molecular conformations generated by the Chemdiv compounds library (Version 2019) were docked to α_{2A}-AR, and the top 100,000 compounds with high affinity were then docked to α_{2B}-AR. The molecular weight distribution of these compounds ranged from 216 Dal to 767 Dal. The binding energy [ChemGauss Score (CGS)] of these compounds to α_{2A}-AR ranged from −22 to −16 kcal/mol, and ranged from −19 to −8 kcal/mol for α_{2B}-AR. A correlation analysis showed that the binding affinity of these compounds for the α_{2A}-AR receptor did not correlate to that for α_{2B}-AR [Figure S1], which made it possible to select the compounds that may bind to α_{2A}-AR with high affinity but not to α_{2B}-AR or with low binding affinity. The binding energies of the selected compounds to α_{2A}-AR or α_{2B}-AR ranged from −22 to −16 kcal/mol or −14 to −8 kcal/mol, respectively. In addition, compound C593–0297 was exceptionally selected with the binding energy −14.85 kcal/mol to α_{2B}-AR [red dot in Figure S1]. Finally, 1023 compounds from the Chemdiv database were screened for druggability filtrates.

2.2. Properties of the Selected Compounds

StarDrop software (6.5.0) was used to analyze the properties of 1023 compounds including water solubility (logS), the lipid–water distribution coefficient (logP), molecular weight, molecular flexibility, the hydrogen bond, the topological polar surface access area, the cytochrome P450 2C9 (CYP2C9) enzyme degradation level, the human *ether-à-go-go-related gene* (hERG) value, oral availability, drug interaction risk (2D6), and other indicators. The summarized score (SS) was calculated based on these properties. The SS values of these compounds ranged from the largest, 0.4379, to the smallest, 0.0023. According to

the SS values, the top 500 compounds with the highest SS scores were selected for the following analysis.

A cluster analysis was performed by a maximum common substructure algorithm to obtain structural diversity of candidate compounds; the similarity threshold was set to 0.5, which divided the 500 compounds into 67 clusters. The correlation plots between the SS scores and other properties such as binding affinity, logS, and logP were analyzed [Figure S2]. By analyzing the structural diversity, binding affinity, and druggability scores, 140 compounds with the best SS values and diverse structures were kept [red in Figure S2A], which were further classified into 21 clusters with an enhanced similarity threshold (0.7) [Figure 1]. Most of the categories contained only two–three compounds, but cluster 2, 4, 11, and 12 contained more compounds. The compounds from cluster 4 and 16 showed high binding affinity to α_{2A}-AR [Figure 1A]. Compared with other clusters, compounds 4 and 10 also bound to α_{2B}-AR [Figure 1B]. Compounds from cluster 7, 9 and 14 may have had lower water solubility [Figure 1C].

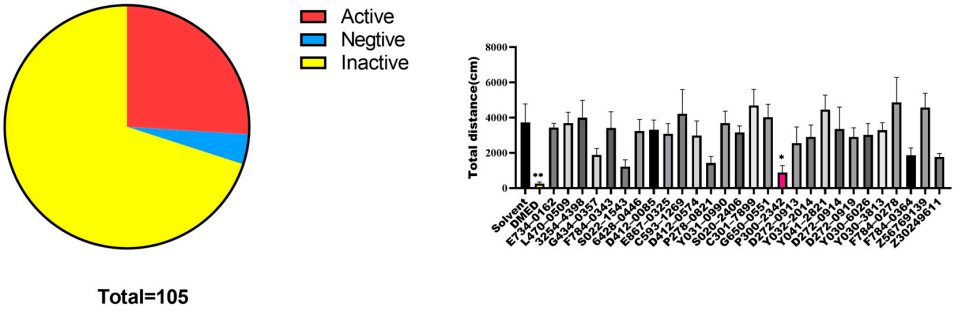


(**A**) (**B**) (**C**)

Figure 1. The properties of 140 compounds in 21 categories. The compounds' affinity to the α2A adrenergic receptor (**A**), α2B adrenergic receptor (**B**), and LogS (**C**) of compounds in 21 categories.

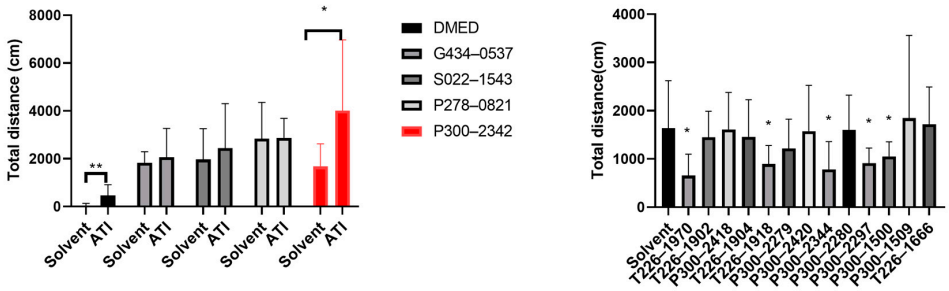
2.3. The Effects of Compounds on the Lorr and Locomotor Activity in Mice

We studied 105 compounds with good druggability in the virtual screening chemicals in the LORR of C57/B6 mice. DMED (432 nmol/kg, i.p.) induced 50% LORR in mice. After intraventricular administration, 28 compounds increased and 4 compounds decreased the percent of LORR induced by DMED (432 nmol/kg, i.p.). A total of 73 compounds displayed no effect on the LORR induced by DMED (432 nmol/kg, i.p.) [Figure 2A]. The 28 compounds (100 nmol/mice, i.c.v.) were further studied for locomotor activity. Among these 28 compounds, 4 compounds significantly inhibited the locomotor activity of mice ($p < 0.05$) [Figure 2B]. Only the inhibition of P300–2342 (10 nmol/mice, i.c.v.) in the mice locomotor activity could be antagonized by the α_2-AR antagonist atipamezole (0.2 mg/kg, i.p.) [Figure 2C]. A total of 13 analogs of P300–2342 were also studied through the locomotor activity of mice. There were five analogs, P300–2344, P300–1500, P300–2297, T226–1918, and T226–1970 (10 nmol/mice, i.c.v.), that inhibited the mice locomotor activity 30–60% compared to that of the solvent [Figure 2D].



(A) **(B)**

Figure 2. *Cont.*



(C) **(D)**

Figure 2. The effects of compounds on the LORR and locomotor activity in mice. (**A**) A total of 105 compounds (100 nmol/mouse, i.c.v.) 15 min prior to DMED administration (432 nmol/kg, i.p.). Twenty-eight compounds increased (active) and four compounds decreased (negative) the percent of LORR induced by DMED (432 nmol/kg, i.p.). Seventy-three compounds displayed no effects (inactive). (**B**) The effect of the active compounds (100 nmol/mouse, i.c.v.) on the locomotor activity of mice. P300–2342 was red. (**C**) The effects of atipamezole (ATI,0.2 mg/kg, i.p.) on the locomotor activity inhibited by four compounds and DMED (10 nmol/mouse, i.c.v.). The red column showed the antagonism of ATI on P300–2342. (**D**) The locomotor activity of mice induced by 13 analogs of P300–2342. n = 8, mean ± SEM, * p< 0.05, ** p < 0.01 compared with the solvent. The analysis was performed using a one-way ANOVA followed by Dunnett's test (**B**,**D**) and a two-way ANOVA followed by Sidak's test (**C**).

2.4. The Interaction of P300–2342 or Analogs with A_{2a}-Ar or A_{2b}-Ar

P300–2342 had affinity for α_{2A}-AR and α_{2B}-AR, inhibiting the binding of [^{3}H] Rauwolscine to the adrenergic receptors with IC_{50} 7.72 ± 0.76 and 12.23 ± 0.11 μM, respectively. The maximum binding inhibition of [^{3}H] Rauwolscine was 83% for α_{2A}-AR and 71% for α_{2B}-AR [Figure 3A,B]. The P300–2342 analogs T226–1970, P300–2344, and P300–1500 concentration-dependently inhibited the binding of [^{3}H] Rauwolscine to α_{2A}-AR with maximum inhibition at 85%, 91%, and 90%, respectively. The half maximal inhibitory concentrations (IC_{50}) of T226–1970, P300–2344, and P300–1500 inhibiting the binding of [^{3}H] Rauwolscine to the α_{2A}-adrenergic receptors were 19.54, 11.34, and 9.66 μM, respectively [Figure 3C]. T226–1970, P300–2344, and P300–1500 also concentration-dependently inhibited the binding of [^{3}H] Rauwolscine to α_{2B}-AR with a maximum inhibition of 94%, 86%, and 85%, respectively, with IC_{50}s of 8.56, 15.91, and 19.05 μM, respectively [Figure 3D]. P300–2297 and T226–1918 had no inhibition on the binding of [^{3}H] Rauwolscine to α_{2A}- or α_{2B}-AR. The α_2 agonists DMED and UK 14304 inhibited the binding of [^{3}H] Rauwolscine to α_{2A}-adrenergic receptors with IC_{50}s of 80.18 and 293.56 nM, respectively. DMED and UK14304 inhibited the binding of [^{3}H] Rauwolscine to α_{2B}-AR with IC_{50} of 14.63 and 550.78 nM, respectively [Figure 3B].

To investigate the binding mode of identified compounds to α_{2A}-AR, the interaction of compounds with α_{2A}-AR were studied using OpenEye software (3.2.0.2). P300–2342 formed a π-hydrogen bond with Y394 in the sixth transmembrane helix and V114 in the third transmembrane helix of α_{2A}-AR with a rigid docking score of –17.47 kcal/mol [Figure 4(A1,A2)]. P300–2342 also formed a π-hydrogen bond with V93 in α_{2B}-AR with a rigid docking score of −11.91 kcal/mol [Figure 4(A3)], which was lower than that of α_{2A}-AR [Figure 4(A2)]. T226–1970 formed one π-hydrogen bond with F390 in the sixth transmembrane helix and two π-hydrogen bonds with L110, V114 in the third transmembrane helix of α_{2A}-AR. The T226–1970 side chain amino formed a hydrogen bond with D113 in the third transmembrane helix of α_{2A}-AR [Figure 4(B1,B2)]. P300–1500 formed π-hydrogen bonds with V114, F390 in the third and sixth transmembrane helix, and formed π-hydrogen bonds with Y196 in extracellular loop2 of α_{2A}-AR. The P300–1500 side chain formed a hydrogen bond with D113 in the third transmembrane helix of α_{2A}-AR [Figure 4(C1,C2)]. P300–2344 formed a π-hydrogen bond with V114 and a hydrogen bond with D113 of α_{2A}-AR [Figure 4(D1,D2)]. T226–1970,

P300–1500, and P300–2344 all formed π-hydrogen bonds with V93 in the C-terminal of the second transmembrane helix of α_{2B}-AR [Figure 4(B3,C3,D3)].

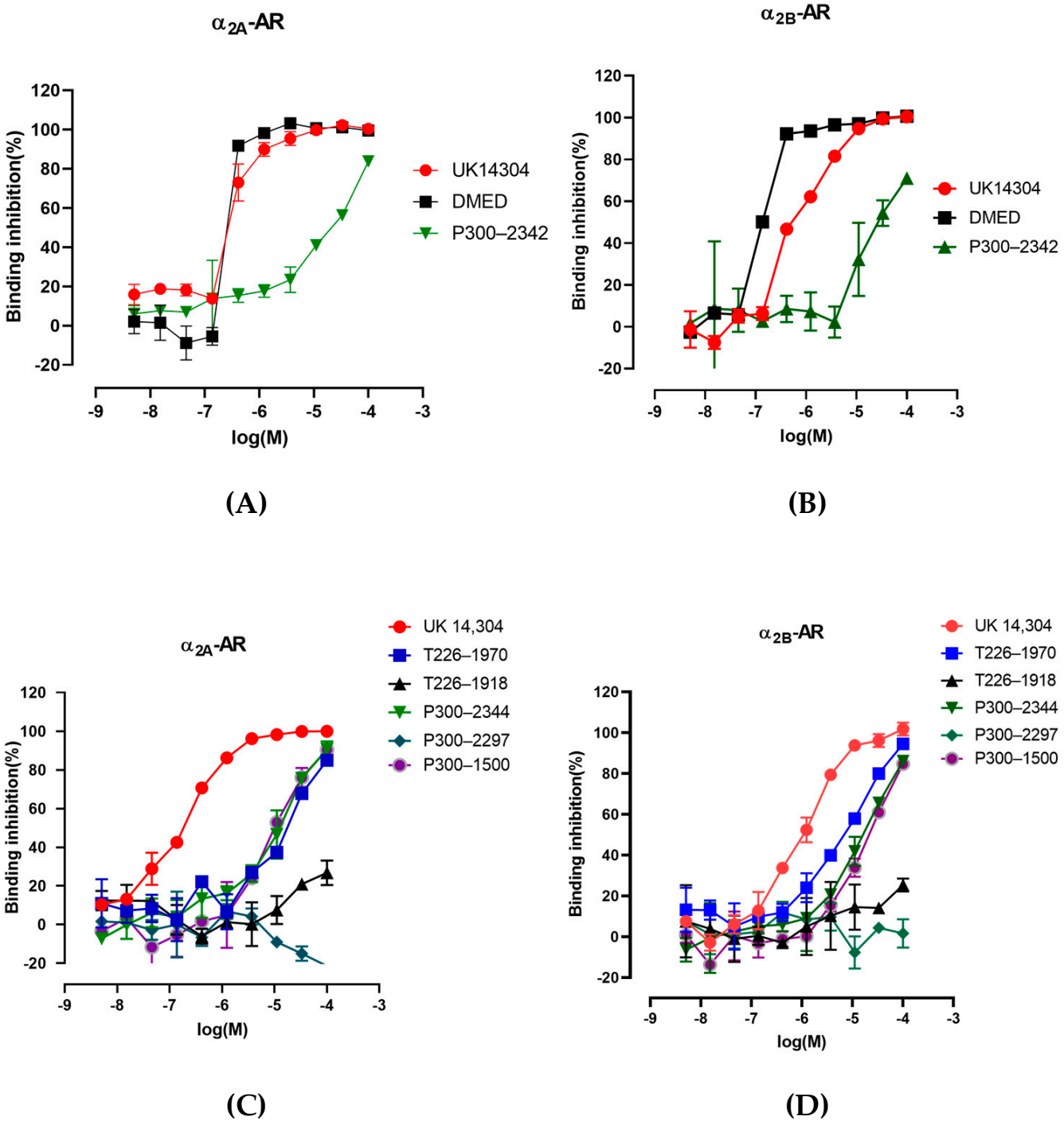


Figure 3. Binding affinities of P300–2342 and its analogs for human α_{2A} and α_{2B}-AR. (**A**) Binding affinities of P300–2342 compared with α_2-AR agonists UK14304 and DMED for human α_{2A}-AR. (**B**) Binding affinities of P300–2342 compared with α_2-AR agonists UK14304 and DMED for human α_{2B}-AR. (**C**) Binding affinities of P300–2342 analogs (T226–1970, T226–1918, P300–2344, P300–2297, P300–1500) compared with α_2-AR agonists UK14304 for human α_{2A}-AR. (**D**) Binding affinities of P300–2342 analogs (T226–1970, T226–1918, P300–2344, P300–2297, P300-1500) compared with α_2-AR agonists UK14304 for human α_{2B}-AR.

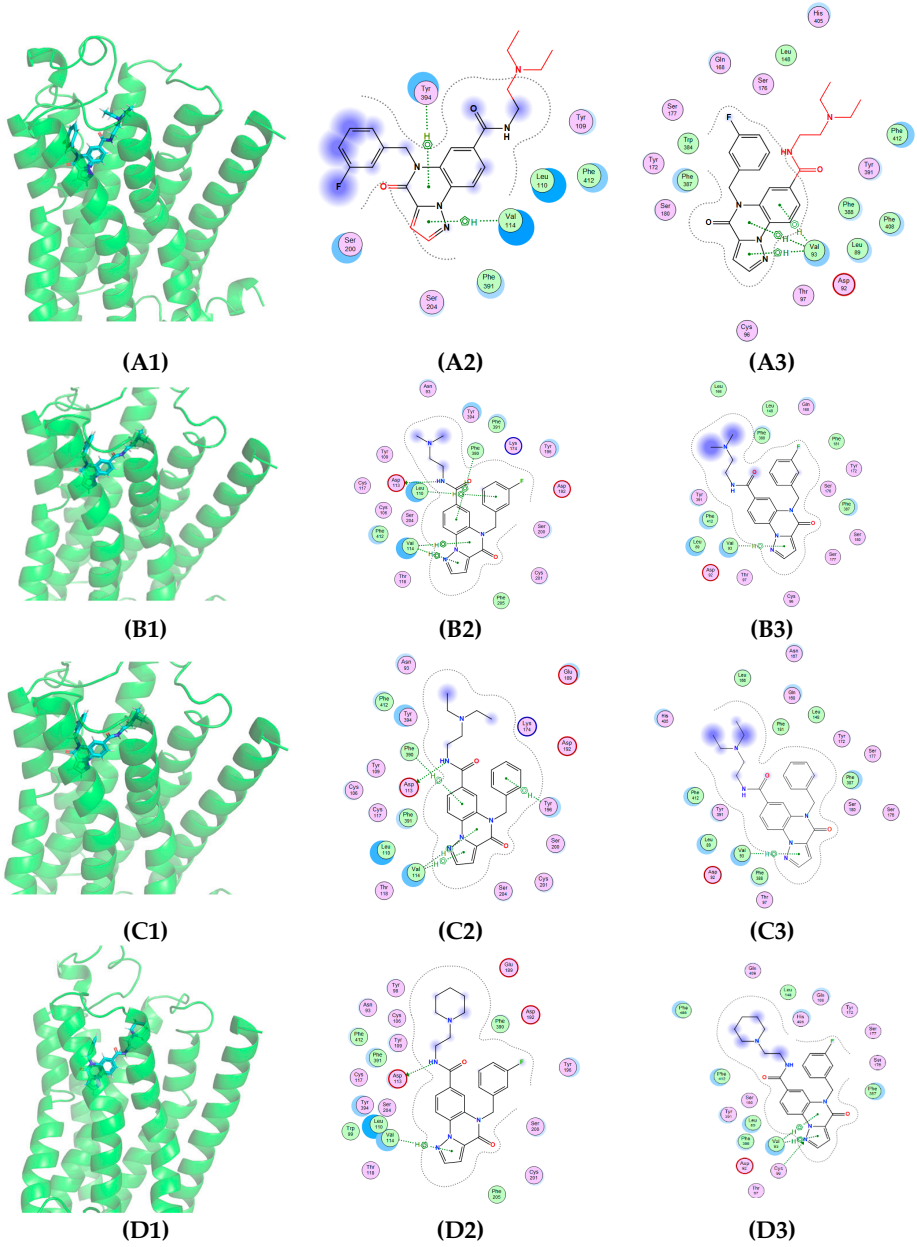


Figure 4. The binding mode of P300–2342 and its analogs to α_{2A} or α_{2B}-AR. (**A1**) The binding mode of P300–2342 with α_{2A}-AR; (**A2**,**A3**) the diagrammatic form of the active sites of the complex P300–2342 with α_{2A} or α_{2B}-AR. (**B1**) The binding mode of T226–1970 with α_{2A}-AR; (**B2**,**B3**) ligand interaction diagram of the complex T226–1970 with α_{2A} or α_{2B}-AR. (**C1**) The binding mode of P300–1500 with α_{2A}-AR; (**C2**,**C3**) the diagrammatic form of the active sites of the complex P300–1500 with α_{2A} or α_{2B}-AR. (**D1**) The binding mode of P300–2344 with α_{2A}-AR; (**D2**,**D3**) The diagrammatic form of the active sites of the complex P300–2344 with α_{2A} or α_{2B}-AR. The hydrogen bonds are indicated by a dotted line. The solvent-accessible surface is indicated by dotted lines. Groups of the compound in the solvent are shown in red. The residual properties are indicated by colors such as purple indicating the polar residues.

2.5. Cyclic Adenosine Monophosphate Assay

In HEK293 cells co-transfected with the pGloSensor-22F cAMP plasmid and pCMV6 Entry-Flag-α_{2A}-AR, DMED (10^{-13}–10^{-9}M) concentration-dependently decreased cAMP accumulation stimulated by forskolin (FSK) (10^{-5}M). In contrast, DMED (10^{-8}–10^{-5}M) concentration-dependently increased cAMP accumulation. P300–2342 (10^{-10}–10^{-5}M)

concentration-dependently decreased cAMP accumulation without increasing cAMP accumulation. The effects of P300–2342 and DMED on the cAMP accumulation were antagonized by the α_{2A}-AR selective antagonist BRL44408 (1 μM). The decrease in cAMP accumulation induced by P300–2342 and DMED was abolished by a 500 ng/mL pretreatment of pertussis toxin (PTX) for 24 h [Figure 5A]. DMED (10^{-10}–10^{-7}M) concentration-dependently increased cAMP accumulation in HEK293 cells transfected with α_{2B}-AR. In contrast, P300–2342 (10^{-10}–10^{-5}M) had no effect on cAMP accumulation [Figure 5B]. P300–2342 formed π-hydrogen bonds with V114 in the third and Y394 in the sixth transmembrane helixes of α_{2A}-AR. In the α_{2A}-AR mutant V114A (α_{2A}V114A-AR), or Y394A (α_{2A}Y394A-AR)-expressed cells, P300–2342 did not decrease cAMP production. Similarly, DMED did not decrease cAMP production in the α_{2A}V114A-AR or α_{2A}Y394A-AR transfected cells. However, DMED increased cAMP production in α_{2A}V114A-AR or α_{2A}Y394A-AR compared to that of α_{2A}-AR wild type [Figure 5C,D]. These results indicated that V114 and Y394 in α_{2A}-AR play important roles in the agonist activation of α_{2A}-AR that couples to the $G_{\alpha i}$ protein.

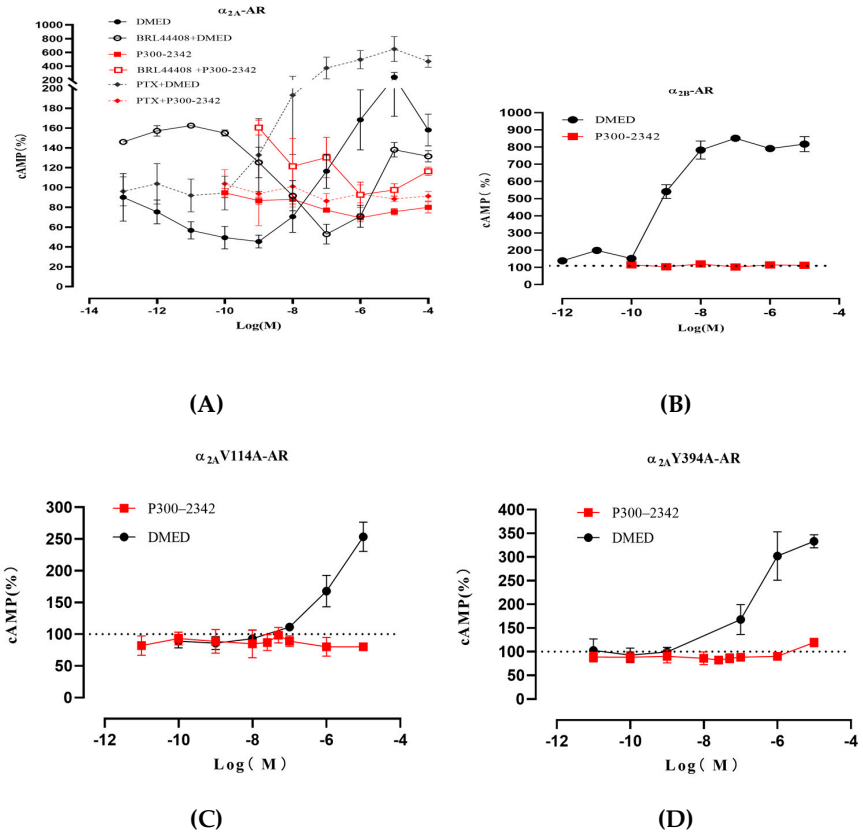
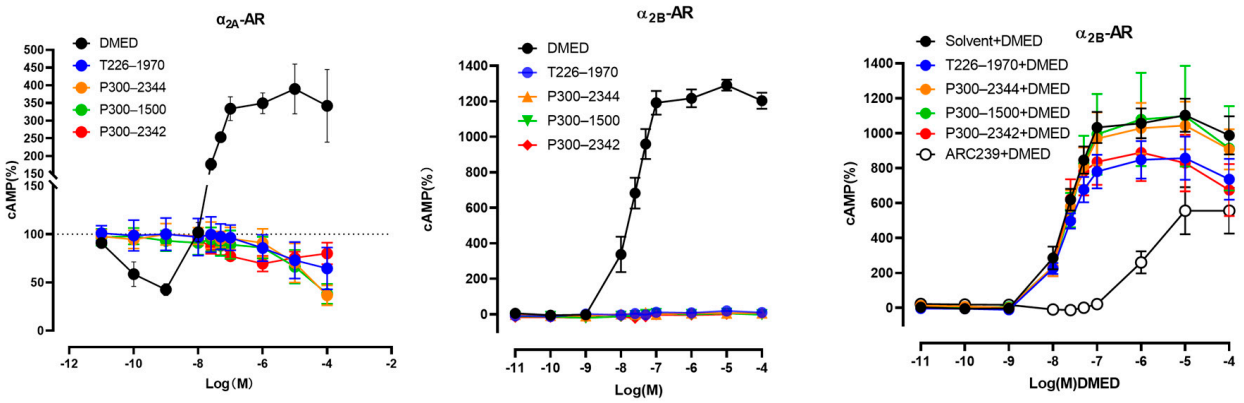


Figure 5. The cAMP production in HEK293 cells transfected with α_{2A}-AR, α_{2B}-AR, or α_{2A}-AR mutants induced by P300–2342. (**A**) HEK293 cells transiently co-transfected with pGloSensor-22F cAMP and pCMV6 Entry-Flag-α_{2A}. The production of cAMP was detected by a time-resolved cAMP measurement assay after P300–2342 or DMED addition without or with BRL44408 pretreatment (1 μM). An amount of 500 ng/mL of pertussis toxin (PTX) was pretreated for 24 h to assay the $G_{\alpha i}$ involvement in the inhibition of AC-cAMP accumulation. (**B**) HEK293 cells transiently co-transfected with pGloSensor-22F cAMP and pCMV6 Entry-Flag-α_{2B}-AR; the production of cAMP was detected after P300–2342 or DMED addition. HEK293 cells transiently co-transfected with pGloSensor-22F cAMP and pCMV6 Entry-Flag-α_{2A}V114A-AR (**C**) or pCMV6 Entry-Flag-α_{2A}Y394A-AR (**D**). the production of cAMP was detected by a time-resolved cAMP measurement assay after P300–2342 or DMED addition; data are shown as the mean ± S.E.M value of three independent experiments performed in triplicate.

As well as P300–2342, the analogs T226–1970, P300–2344, and P300–1500 decreased cAMP production without increasing cAMP accumulation in α_{2A}-AR-HEK293 cells [Figure 6A]. T226–1970, P300–2344, and P300–1500 also had no activation in α_{2B}-AR [Figure 6B]. In α_{2B}-AR-HEK293 cells, the α_{2B}-AR selective antagonist ARC239 (10 μM) decreased the cAMP accumulation induced by DMED and made the dose–response curve shift to the right. P300–2342 and T226–1970 (10 μM) slightly decreased the cAMP accumulation induced by DMED, whereas P300–2344 and P300–1500 (10 μM) had no effects on the DMED-stimulated cAMP [Figure 6C].



(A) **(B)** **(C)**

Figure 6. The cAMP production in HEK293 cells transfected α_{2A}-AR or α_{2B}-AR induced by P300–2342 analogs. (**A**) HEK293 cells transiently co-transfected with pGloSensor-22F cAMP and pCMV6 Entry-Flag-α_{2A}-AR; the production of cAMP was detected by a time-resolved cAMP measurement assay after T226–1970, P300–2344, P300–1500, P300–2342, or DMED addition. (**B**) HEK293 cells transiently co-transfected with pGloSensor-22F cAMP and pCMV6 Entry-Flag-α_{2B}-AR. The production of cAMP was detected by a time-resolved cAMP measurement assay after T226–1970, P300–2344, P300–1500, P300–2342, or DMED addition. (**C**) The effects of T226–1970, P300–2344, P300–1500, and P300–2342 pretreatment on the cAMP accumulation induced by DMED in pGloSensor-22F cAMP and pCMV6 Entry-Flag-α_{2B}-AR co-transfected cells.

3. Discussion

The selective α_2-AR subtype antagonist and α_2-AR subtype knockout mice demonstrated α_{2A}-AR-subtype-mediated sedation induced by α_2-AR agonists [16]. Presynaptic α_{2A}-AR activation of Gi/o can inhibit the activity of adenylate cyclase with the attenuation of cAMP production, activation of K^+ conduction, acceleration of Na^+/H^+ exchange, and inhibition of Ca^{2+} channels [17]. As the classic GPCR, α_{2A}-AR has seven transmembrane segments, three extracellular loops, and three intracellular loops. Each transmembrane segment consists of 20 to 26 amino acids forming an α helix, in which the hydrophobic amino acids form a "pocket", which determines the specificity of binding to the ligand. The second and third intracellular loops are related to the G protein coupling of the receptor. The N-terminal part of the third intracellular loop and some amino acid residues of the second intracellular loop determine the specificity of the interaction between the receptor and the G protein. The C-terminal part of the third intracellular loop is also involved in the interaction between the receptor and the G protein, but it is mainly related to the coupling efficiency of the receptor and the G protein [11,18].

The Chemdiv database (Version 2019), containing 1,535,478 small molecule compounds with diverse backbones, was used for virtual screening. To ensure the global conformation of small molecules in the virtual screening process, the plug-in omega in OpenEye software was used to generate small molecule conformations. On average, each small molecule generated about 50 conformations. We converted the Chemdiv molecules into

50,679,311 molecular conformations and docked the compounds with α_{2A}-AR crystal structures, and the top 100,000 were then docked to α_{2B}-AR crystal structures. There was no obvious correlation in the compound affinities to α_{2A}-AR and α_{2B}-AR [Figure S1]. The Chemdiv database binding the α_{2A}-AR receptor with high affinity but with low binding affinity to α_{2B}-AR allowed us to select 1023 compounds for property analysis. The 500 compounds with the highest SS scores (logS, logP, molecular weight, molecular flexibility, hydrogen bond, topological polar surface area (TPSA), CYP2C9 degradation, hERG inhibition, HIA, 2D6, etc.) were selected for structural diversity analysis. The 140 compounds with the best SS values and diverse structures were further classified into 21 categories with an enhanced similarity threshold (0.7) [Figure 1].

In our study, approximately three quarters of the 105 compounds with the best SS values had no sedation or anti-sedative effects, one quarter of the compounds had sedative effects, and a few compounds had anti-sedative effects [Figure 2A, Table S1]. Most of the small molecular compounds interacted with D113 in the third transmembrane helix and E189 in the second extracellular loop. At the same time, N93 and V114 were also involved in the binding of most compounds. In addition, 17 amino acid sites, including W99, C106, Y109, C117, T118, S165, C188, I190, D192, Y196, S200, F390, F391, Y394, K409, F412, and Y416, were involved in the interaction of the compounds and α_{2A}-AR in the present study. D113 in the third transmembrane domain (TM3) is the conservative ligand-contacting residue in the aminergic receptor including α_1, α_2, and the β adrenergic receptor [19]. D113N inhibits the binding of [^{3}H] yohimbine to α_2-adrenergic receptors with a small decrease in cAMP accumulation stimulated by forskolin and the potentiation of forskolin-stimulated cAMP accumulation [13]. S200 in the fifth transmembrane domain (TM5) of hα_2-AR involved in the ligand binding pocket plays an important role in epinephrine and UK-14304 binding and response [13,20]. Qu et al. found twelve residues (D113, V114, S200, C201, S204, W387, F390, F391, Y394, F408, F412, and Y416) involved in the binding pocket of α_{2A}-AR by a co-crystallized partial agonist and antagonist. These four residues, D113, F390, F412, and Y416, are involved in the formation of an aromatic cage in both α_{2A}-AR and α_{2B}-AR [14]. In our study, Y394 in α_{2A}-AR formed a π-hydrogen bond with an imidazoline ring in compound P300–2342. Y394 formed hydrogen bonds with the α_{2A}-AR agonists epinephrine, norepinephrine, and UK14,304 [14]. V114 in the third transmembrane helix of α_{2A}-AR also formed a π-hydrogen bond with a phenyl ring in P300–2342. P300–2342 also formed a π-hydrogen bond with Val93 in α_{2B}-AR receptors (Figure 4(A3)).

Similar to previous reports, α_{2A}-AR wild type (WT) simultaneously coupled to both the Gi and Gs proteins [21] when stimulated by the agonists UK14,304 and DMED (Figure 5A). However, α_{2A}-AR WT activated by P300–2342 only coupled to Gi proteins (Figures 5A and 6A). In contrast to α_{2A}-AR and Y394N in previous reports [14], the mutant α_{2A}-AR Y394A lost the coupling to Gi proteins and only coupled to Gs proteins with DMED treatment [Figure 5D]. In the epinephrine-bound β2-AR, epinephrine formed hydrogen bonds with S204 and N293 (6.55), which play an important role in the Gs activation of β2-AR. N293 is relative to Y394 (6.55) in α_{2A}-AR [22]. The polar amino acids Y394 or N394 in α_{2A}-AR are important to Gi protein signals under agonist addition. In contrast, the nonpolar amino acid A394 mutant α_{2A}-AR only activated Gs protein signals in our study.

GPCR signaling is well-demonstrated according to the progress in GPCR structural biology. The GPCR cytoplasmic end of the seven transmembrane helix domain is closed in the inactive states [23,24]. The sixth transmembrane helix plays an important role in GPCR-Gi activation [25–27]. In the present study, α_{2A}-AR Y394A in the mutant sixth transmembrane helix lost Gi protein activation upon agonist addition, in accordance with the previous view. Except for the amino in transmembrane helix 6, the three serines (S200, S201, and S204) in transmembrane helix 5 and D130 in transmembrane helix 3 are involved in the agonist interaction with β2-AR [22,28,29]. These amino acids are also involved in α_2-AR interactions with catecholamines [30], which might play an important role in Gs protein coupling. P300–2342 formed a π-hydrogen bond with Y394 in the sixth transmembrane helix and V114 in the third transmembrane helix in the binding

pockets of α_{2A}-AR. The interaction between P300–2342 and α_{2A}-AR could not make the receptor couple to the Gs protein. Consistent with the α_{2A}-ARY394A mutant, α_{2A}-AR V114A only coupled to Gs proteins after DMED addition [Figure 6C]. P300–2342 lost its coupling to Gi proteins in α_{2A}-AR, Y394A, α_{2A}-AR, and the V114A mutant, which indicated that V114 in the third and Y394 in the sixth transmembrane helixes play important roles in Gi protein coupling (Figure 6C,D). Although P300–2342 formed a π-hydrogen bond with V93 in α_{2B}-AR and inhibited the binding of [^{3}H] Rauwolscine to α_{2B}-AR, P300–2342 had no activation in α_{2B}-AR coupling to Gs proteins. V93 is a conserved site in α_1, α_2, and β-AR [15]. Yuan et al. found V93 in the third transmembrane helix involved in the binding pocket of DMED in α_{2B}-AR, but V93 had no interaction with DMED [15]. V93 might not to be the key site for the agonist activation. The P300–2342 interacting sites Y394, V114 in α_{2A}-AR, and V93 in α_{2B}-AR contributed to the uncoupling to Gs proteins, which prevented the unwanted Gs coupling activity. The P300–2342 analogs T226–1970, P300–2344, and P300–1500 also formed π-hydrogen bonds or hydrogen bonds with α_{2A}-AR and α_{2B}-AR, and then inhibited the binding of [^{3}H] Rauwolscine to α_{2A}-AR and α_{2B}-AR. α_{2A}-AR only coupled to Gi proteins following the activation of three analogs of P300–2342. T226–1970, P300–2344, and P300–1500 also had no activation to α_{2B}-AR (Figure 6B). The structure of P300–2342 and the three analogs is more complex than that of the α_{2A}-AR agonists like epinephrine, dexmedetomidine, and clonidine [Figure 2]. These compounds were also larger than the α_{2A}-AR full agonist UK14304. P300–2342 and its analogs had several benzene moieties with a long polar residue. These large molecular compounds were hydrophobic and obstructed the interaction with the residues in α_{2A}-AR. Therefore, α_{2A}-AR could not couple to Gs proteins after being activated by P300–2342 and its analogs. P300–2342 and its analogs could serve as lead compounds with sedative effects without the vascular side effects. We speculate that the future development of compounds capable of selectively activating α_{2A}-AR while blocking α_{2B}-AR may further improve our capability to treat hypertension, ischemic heart disease, and heart failure.

4. Conclusions

Most α_2-AR agonists are imidazole ring compounds that have no selectivity for $\alpha_{2A/2B}$-AR or Gi/Gs, potentially resulting in drug side effects. In this study, we performed a structure-based virtual screening strategy to identify the selective α_{2A}-AR agonists. We used virtual screening and druggability filtering for the ChemDiv library. We found that 1023 compounds may bind to α_{2A}-AR with high affinity but with low affinity to α_{2B}-AR. Among them, 105 compounds with good druggability according to virtual screening were purchased and studied in the LORR of C57/B6 mice. Ligand binding assays showed that compound P300–2342 selectively activated α_{2A}-AR, and the cAMP assay indicated that P300–2342 could only couple to the Gi/o protein signaling pathway for sedation. Compound P300–2342 may serve as a lead compound for sedatives by activation of α_{2A}-AR with potentially few side effects. Our research can provide a basis for developing novel selective agonists.

5. Materials and Methods

5.1. Protein Preparation for Humanα_2-AR Proteins and Binding Pocket Identification

The 3D structure of α_{2A}-AR in complex with a partial agonist E39 (pdbid:6kuy) is shown in Figure S3A, where the ligand binding area is in the extracellular domain. The ligand binding area contained four adjacent hydrophobic pockets [Figure S4A]. Similarly, the 3D structure of α_{2B}-AR in complex with agonist DMED (pdbid:6k42) is shown in Figure S3B, with seven transmembrane regions and an extracellular domain, which was highly similar to the structure of α_{2A}-AR subtype (all atoms RMSD = 4.27 Å). The ligand-binding site was located in the extracellular domain, which is consistent with the ligand-binding region of the α_{2A}-AR subtype. Two adjacent molecular binding pockets were selected at the ligand site in crystal structures by the MOE package [Figure S4B]. In order to identify the compounds which could specifically bind to the α_{2A}-AR subtype but not α_{2B}-

AR, the relevant pockets from both subtypes were chosen to perform the structure-based virtual screening.

5.2. Virtual Screening

The crystal structure of α_{2A}-AR and α_{2B}-AR were protonated and optimized by MOE QuickPrep (2019.0102). The optimized structures were then converted to the formatted receptor files that defined all the above-mentioned residues as the docking area by using the appropriate (apopdb2receptor) module of OpenEye software (Release 3.2.0.2). The docking areas of α_{2A}-AR and α_{2B}-AR were a rectangle with a box size of 27.67 Å × 19.33Å × 22.33 Å and 28.00 Å × 23.67 Å × 23.67 Å, respectively.

The Chemdiv compound library was selected for virtual screening, which contained 1,535,478 compounds. FRED performs rigid docking, so OMEGA2 was used with all default parameters to search for as many conformations as possible for each compound. OEDocking (Release 3.0) was used to dock all conformations of compounds to α_{2A}-AR, with the parameters -save_component_scores: true; -hitlist_size: 100,000; -docked_molecule_file: sdf. The top 100,000 compounds for α_{2A}-AR were docked to the binding pocket of α_{2B}-AR, and multiple conformations were also generated by OMEGA. StarDrop (Release 6.6.4) was used to calculate the structural diversity based on a maximum common substructure algorithm to cluster compounds containing a significant common substructure. The molecular properties such as logS, HIA category, logP, hERG, 2D6, 2C9 affinity, P-gp category, PPB90, and BBB permeability were used as a scoring function to evaluate the druggability of each molecule.

5.3. Loss of Righting Reflex (LORR) and Locomotor Activity

5.3.1. Materials

C57BL/6 mice (20–22 g) were purchased from the SPF biotechnology co., LTD (Beijing, China). All the animals were housed in an alternating 12 h light/12 h dark cycle room, which was maintained in a climate-controlled environment (25 ± 1 °C). Animals had free access to water and food. All the experimental procedures were reviewed and approved by the ethics committee and institutional animal care and use committee of the Beijing Institute of Pharmacology and Toxicology, Beijing, China (IACUC of AMMS–06–2017–001). Animals were assigned to groups randomly before testing. Testing occurred within the same approximate time of day between experiments. The experimenter was blinded to treatment throughout the course of behavioral testing.

Drugs were purchased from various vendors. Dexmedetomidine was purchased from (Dexinjia Biotechnology, Jinan, China). BRL44408 was purchased from (Sigma, Louis, MO, USA). Forskolin was purchased from (Sigma, Louis, MO, USA). UK 14,304 was purchased from (Tocris, Bristol, UK). [^{3}H] Rauwolscine was purchased from (PerkinElmer, Waltham, MA, USA). The selected compounds were purchased from (Topscience, Shanghai, China). Dexmedetomidine and BRL44408 were dissolved in sterile physiological saline (0.9% NaCl) to the final concentration used in this study. The selected compounds were dissolved in 5% DMSO.

5.3.2. LORR and Locomotor Activity

The LORR in C57/B6 mice were used to study the effects of screening compounds. Mice were pre-treated with compounds (100 nmol/mouse, i.c.v.) 15 min prior to DMED administration (432 nmol/kg, i.p.). The righting reflex was deemed to be "lost" if the mouse failed to right itself within 60 s of being placed on its back, as described in our previous study [31]. The effects of the compounds on the spontaneous locomotor activity of mice were detected using a LabState video tracking system (Anilab Scientific Instruments Co., Ltd., Ningbo, China). The mice were placed in acrylic boxes (40 cm × 40 cm × 35 cm) for 30–60 min before compound treatment on day 1. On day 2, compounds (10 or 100 nmol) were injected into the cerebral ventricles (i.c.v.) of the mice 30 min before being placed in acrylic boxes. The locomotor activity of each mouse was defined by the horizontal distance it travelled (in centimeters) over 30–60 min [32].

5.4. Ligand-Binding Assay

The competitive inhibition of [^{3}H] Rauwolscine (2.5 nmol/L) binding to human α_{2A}-AR or α_{2B}-AR was performed in the presence of various concentrations of P300–2342, T226–1970, T226–1918, P300–2344, P300–2297, P300–1500, UK 14304, and DMED. CHO-K1 cells expressing human α_{2A}-AR or α_{2B}-AR membranes (2 μg, ES-030-M400UA/NET722250UC, PerkinElmer) were incubated at 27 °C for 1 h in 50 mM Tris-HCl, 1 mM EDTA buffer with 2.5 nM [^{3}H] Rauwolscine in the presence or absence of ten concentrations of competing ligands ranging from 1.3×10^{-9} to 1.0×10^{-4}. The reactions were transferred to the pretreated UNIFILTER-96 GF/B plates (PerkinElmer) and rinsed four times with 50 mM Tris-HCl by Universal Harvest (PerkinElmer). The plates were dried at 55 °C for 10 min, and 40 μL ULTIMA GOLD (PerkinElmer) scintillation fluid was added to each well. Radioactivity retained in each sample was counted in a Microbeta2 (PerkinElmer). The binding inhibition % = (average value of negative control-CPM)/(average value of negative control-average value of positive control) × 100.

5.5. cAMP Assay

According to the GloSensor cAMP biosensor (Promega, Shanghai, China) manufacturer protocols, HEK293 cells were co-transfected with the pGloSensor-22F cAMP plasmid (Promega, E1171) and pCMV6 Entry-Flag-α_{2A}-AR. After 24 h, the cells were seeded in white 96-well plates. The next day, the cell media were replaced by 90 μL of fresh DMEM with 2% v/v GloSensor cAMP reagent (Promega, E1290) and incubated for 60 min at 37 °C. Before drug stimulation, an initial measurement of the baseline signal was detected. Then cells were stimulated with 10^{-12}, M-10^{-5}, M, P300–2342, T226–1970, P300–2344, P300–1500, or DMED for 10 min and then were stimulated with forskolin (10 μM) for 15 min with or without α_{2A}-AR antagonist BRL44408 (10 μM) pretreatment. PTX 500 ng/mL selectively ablated receptor Gi coupling [32]. PTX 500 ng/mL pretreatment for 24 h was used to assay the chemical effects on Gi coupling following α_{2A}-AR activation. Two mutations, V114A and Y394A were introduced into the α_{2A}-AR genes, respectively, using standard QuickChange PCR. The cAMP accumulations induced by DMED or P300–2342 were also studied in HEK293 cells co-transfected with the pGloSensor-22F cAMP plasmid and pCMV6 Entry-Flag-α_{2A}V114A-AR or α_{2A}Y394A-AR with forskolin (10 μM) stimulation. HEK293 cells co-transfected with the pGloSensor-22F cAMP plasmid and pCMV6 Entry-Flag-α_{2B}-AR were stimulated with P300–2342, T226–1970, P300–2344, P300–1500, or DMED to detect the cAMP accumulation. In each experiment, the cAMP assay used pcDNA3.1 myc/hisB transfected cells as a negative control and cells stimulated with 10 μM of forskolin as a positive control. The signal was read using a Victor 2D Instrument (PerkinElmer) at 675 nm. The production of cAMP% was calculated (the signal value after chemicals addition–baseline signal value)/the baseline signal value *100 as described in our previous study [33].

Supplementary Materials: The following supporting information can be downloaded at: https://www.mdpi.com/article/10.3390/ijms25137233/s1.

Author Contributions: Conceptualization, P.Z. and R.S.; methodology, F.L.; software, S.S.; validation, H.Z., B.S. and X.W.; formal analysis, R.S.; investigation, P.Z.; resources, Y.L. data curation, P.Z.; writing—original draft preparation, P.Z.; writing—review and editing, R.S.; project administration, P.Z.; funding acquisition, P.Z. All authors have read and agreed to the published version of the manuscript.

Funding: This research was funded by the National Natural Science Foundation of China, grant number 82273909 by P.Z.

Institutional Review Board Statement: The animal study protocol was approved by the ethics committee and Institutional Animal Care and Use Committee of the Beijing Institute of Pharmacology and Toxicology, Beijing, China (IACUC of AMMS-06–2017-001).

Informed Consent Statement: Not applicable.

Data Availability Statement: Data are contained within the article and Supplementary Materials.

Acknowledgments: The authors acknowledge Jiangfeng Du (Zhengzhou University) for the data analysis by using Stardrop and MOE software and Zhibin Zheng (Beijing Institute of Pharmacology and Toxicology) for the chemicals analysis.

Conflicts of Interest: The authors declare no conflicts of interest. The funders had no role in the design of the study; in the collection, analyses, or interpretation of data; in the writing of the manuscript; or in the decision to publish the results.

References

1. Delmas, P.; Abogadie, F.C.; Milligan, G.; Buckley, N.J.; Brown, D.A. Betagamma dimers derived from Go and Gi proteins contribute different components of adrenergic inhibition of Ca^{2+} channels in rat sympathetic neurons. *J. Physiol.* **1999**, *518*, 23–36. [CrossRef] [PubMed]
2. Scheinin, M.; Lomasney, J.W.; Hayden-Hixson, D.M.; Schambra, U.B.; Caron, M.G.; Lefkowitz, R.J.; Fremeau, R., Jr. Distribution of a2-adrenergic receptor subtype gene expression in rat brain. *Brain Res. Mol. Brain Res.* **1994**, *21*, 133–149. [CrossRef] [PubMed]
3. MacDonald, E.; Kobilka, B.K.; Scheinin, M. Gene targeting–homing in on alpha 2-adrenoceptor-subtype function. *Trends Pharmacol. Sci.* **1997**, *18*, 211–219. [CrossRef] [PubMed]
4. Gavras, I.; Manolis, A.J.; Gavras, H. The alpha2 -adrenergic receptors in hypertension and heart failure: Experimental and clinical studies. *J. Hypertens.* **2001**, *19*, 2115–2124. [CrossRef] [PubMed]
5. Timmermans, P.B.; van Zwieten, P.A. Mini-review. The postsynaptic alpha 2-adrenoreceptor. *J. Auton. Pharmacol.* **1981**, *1*, 171–183. [CrossRef] [PubMed]
6. Van Meel, J.C.; De Jonge, A.; Kalkman, H.O.; Wilffert, B.; Timmermans, P.B.; Van Zwieten, P.A. Vascular smooth muscle contraction intiated by postsynaptic alpha2-adrenoceptor activation is induced by an influx of extracellular calcium. *Eur. J. Pharmacol.* **1981**, *69*, 205–208. [CrossRef] [PubMed]
7. Link, R.E.; Desai, K.; Hein, L.; Stevens, M.E.; Chruscinski, A.; Bernstein, D.; Barsh, G.S.; Kobilka, B.K. Cardiovascular regulation in mice lacking alpha2-adrenergic receptor subtypes b and c. *Science* **1996**, *273*, 803–805. [CrossRef] [PubMed]
8. Makaritsis, K.P.; Handy, D.E.; Johns, C.; Kobilka, B.; Gavras, I.; Gavras, H. Role of the alpha2B-adrenergic receptor in the development of salt-induced hypertension. *Hypertension* **1999**, *33*, 14–17. [CrossRef]
9. Ekaterina Kintsurashvili, E.; Johns, C.; Ignjacev, I.; Gavras, I.; Gavras, H. Central alpha2B-adrenergic receptor antisense in plasmid vector prolongs reversal of salt-dependent hypertension. *J. Hypertens.* **2003**, *21*, 961–967. [CrossRef]
10. Hein, L.; Altman, J.D.; Kobilka, B.K. Two functionally distinct alpha2-adrenergic receptors regulate sympathetic neurotransmission. *Nature* **1999**, *402*, 181–184. [CrossRef]
11. Eason, M.G.; Liggett, S.B. Identification of a Gs coupling domain in the amino terminus of the third intracellular loop of the alpha 2A-adrenergic receptor. Evidence for distinct structural determinants that confer Gs versus Gi coupling. *J. Biol. Chem.* **1995**, *270*, 24753–24760. [CrossRef] [PubMed]
12. Correa-Sales, C.; Reid, K.; Maze, M. Pertussis toxin-mediated ribosylation of G proteins blocks the hypnotic response to an alpha 2-agonist in the locus coeruleus of the rat. *Pharmacol. Biochem. Behav.* **1992**, *43*, 723–727. [CrossRef] [PubMed]
13. Wang, C.D.; Buck, M.A.; Fraser, C.M. Site-directed mutagenesis of alpha 2A-adrenergic receptors: Identification of amino acids involved in ligand binding and receptor activation by agonists. *Mol. Pharmacol.* **1991**, *40*, 168–179. [PubMed]
14. Qu, L.; Zhou, Q.T.; Xu, Y.M.; Guo, Y.; Xiaoyu Chen, X.Y.; Yao, D.Q.; Gye Won Han, G.H.; Zhi-Jie Liu, Z.J.; Stevens, R.C.; Zhong, G.S.; et al. Structural Basis of the Diversity of Adrenergic Receptors. *Cell Rep.* **2019**, *29*, 2929–2935. [CrossRef] [PubMed]
15. Yuan, D.; Liu, Z.; Kaindl, J.; Maeda, S.; Zhao, J.; Sun, X.; Xu, J.; Gmeiner, P.; Wang, H.W.; Kobilka, B.K. Activation of the α 2B adrenoceptor by the sedative sympatholytic dexmedetomidine. *Nat. Chem. Biol.* **2020**, *16*, 507–512. [CrossRef] [PubMed]
16. Lakhlani, P.P.; MacMillan, L.B.; Guo, T.Z.; McCool, B.A.; Lovinger, D.M.; Maze, M.; Limbird, L.E. Substitution of a mutant alpha2a-adrenergic receptor via "hit and run" gene targeting reveals the role of this subtype in sedative, analgesic, and anesthetic-sparing responses in vivo. *Proc. Natl. Acad. Sci. USA* **1997**, *94*, 9950–9955. [CrossRef] [PubMed]
17. Limbird, L.E. Receptors linked to inhibition of adenylate cyclase: Additional signaling mechanisms. *FASEB J.* **1988**, *2*, 2686–2695. [CrossRef] [PubMed]
18. Insel, P.A. Seminars in medicine of the Beth Israel Hospital, Boston. Adrenergic receptors–evolving concepts and clinical implications. *N. Engl. J. Med.* **1996**, *334*, 580–585. [CrossRef] [PubMed]
19. Michino, M.; Beuming, T.; Donthamsetti, P.; Newman, A.H.; Javitch, J.A.; Shi, L. What can crystal structures of aminergic receptors tell us about designing subtype-selective ligands? *Pharmacol. Rev.* **2015**, *67*, 198–213. [CrossRef] [PubMed]
20. Marjamaki, A.; Pihlavisto, M.; Cockcroft, V.; Heinonen, P.; Savola, J.M.; Scheinin, M. Chloroethylclonidine binds irreversibly to exposed cysteines in the fifth membrane-spanning domain of the human alpha2A-adrenergic receptor. *Mol. Pharmacol.* **1998**, *53*, 370–376. [CrossRef]
21. Eason, M.G.; Kurose, H.; Holt, B.D.; Raymond, J.R.; Liggett, S.B. Simultaneous coupling of alpha 2-adrenergic receptors to two G-proteins with opposing effects. Subtype-selective coupling of alpha 2C10, alpha 2C4, and alpha 2C2 adrenergic receptors to Gi and Gs. *J. Biol. Chem.* **1992**, *267*, 15795–15801. [CrossRef] [PubMed]

22. Masureel, M.; Zou, Y.; Picard, L.P.; van derWesthuizen, E.; Mahoney, J.P.; Rodrigues, J.P.G.L.M.; Mildorf, T.J.; Dror, R.O.; Shaw, D.E.; Bouvier, M.; et al. Structural insights into binding specificity, efficacy and bias of a b2AR partial agonist. *Nat. Chem. Biol.* **2018**, *14*, 1059–1066. [CrossRef] [PubMed]
23. Cherezov, V.; Rosenbaum, D.M.; Hanson, M.A.; Rasmussen, S.G.F.; Thian, F.S.; Kobilka, T.S.; Choi, H.J.; Kuhn, P.; Weis, W.I.; Kobilka, B.K.; et al. High-resolution crystal structure of an engineered human β2-adrenergic G protein-coupled receptor. *Science* **2007**, *318*, 1258–1265. [CrossRef] [PubMed]
24. Rosenbaum, D.M.; Cherezov, V.; Hanson, M.A.; Rasmussen, S.G.F.; Thian, F.S.; Kobilka, T.S.; Choi, H.J.; Yao, X.J.; Weis, W.I.; Stevens, R.C.; et al. GPCR engineering yields high-resolution structural insights into beta2-adrenergic receptor function. *Science* **2007**, *318*, 1266–1273. [CrossRef] [PubMed]
25. Kang, Y.; Kuybeda, O.; de Waal, P.W.; Mukherjee, S.; Van Eps, N.; Dutka, P.; Zhou, X.E.; Bartesaghi, A.; Erramilli, S.; Morizumi, T.; et al. Cryo-EM structure of human rhodopsin bound to an inhibitory G protein. *Nature* **2018**, *558*, 553–558. [CrossRef] [PubMed]
26. Draper-Joyce, C.J.; Khoshouei, M.; Thal, D.M.; Liang, Y.L.; Nguyen, A.T.N.; Furness, S.G.B.; Venugopal, H.; Baltos, J.A.; Plitzko, J.M.; Danev, R.; et al. Structure of the adenosine-bound human adenosine A1 receptor-Gicomplex. *Nature* **2018**, *558*, 559–563. [CrossRef] [PubMed]
27. Kang, Y.; Kuybeda, O.; de Waal, P.W.; Mukherjee, S.; Van Eps, N.; Koehl, A.; Hu, H.; Maeda, S.; Zhang, Y.; Qu, Q.; et al. Structure of the mu-opioid receptor-Gi protein complex. *Nature* **2018**, *558*, 547–552.
28. Warne, T.; Moukhametzianov, R.; Baker, J.G.; Nehme', R.; Edwards, P.C.; Le-slie, A.G.; Schertler, G.F.; Tate, C.G. The structural basis foragonist and partial agonist action on a β(1)-adrenergic receptor. *Nature* **2011**, *469*, 241–244. [CrossRef] [PubMed]
29. Moukhametzianov, R.; Warne, T.; Edwards, P.C.; Serrano-Vega, M.J.; Leslie, A.G.; Tate, C.G.; Schertler, G.F. Two distinct conformations of helix 6 observed in antagonist-bound structures of a beta1-adrenergic receptor. *Proc. Natl. Acad. Sci. USA* **2011**, *108*, 8228–8232. [CrossRef]
30. Ostopovici-Halip, L.; Curpăn, R.; Mracec, M.; Bologa, C.G. Structural determinants of the alpha2 adrenoceptor subtype selectivity. *J. Mol. Graph. Model.* **2011**, *29*, 1030–1038. [CrossRef]
31. Liu, M.; Yang, Y.; Tan, B.; Li, Y.L.; Zhou, P.L.; Su, R.B. G αi and G βγ subunits have opposing effects on dexmedetomidine-induced sedation. *Eur. J. Pharmacol.* **2018**, *831*, 28–37. [CrossRef] [PubMed]
32. Li, K.; Liu, X.; Zhang, M.; Su, R. Effects of Ketanserin, M100907 and Olanzapine on hallucinogenic like action induced by 2, 5-dimethoxy-4-methylamphetamine. *Behav. Pharmacol.* **2023**, *34*, 92–100. [CrossRef] [PubMed]
33. Zhu, H.; Liu, X.; Wang, X.; Li, Y.; Ma, F.; Tan, B.; Zhou, P.; Fu, F.; Su, R. Gβγ subunits inhibitor decreased head twitch response induced by DOM through the PLCβ/IP3/Ca^{2+}/ERK and cAMP signaling pathways. *Eur. J. Pharmacol.* **2023**, *957*, 176038. [CrossRef] [PubMed]

Disclaimer/Publisher's Note: The statements, opinions and data contained in all publications are solely those of the individual author(s) and contributor(s) and not of MDPI and/or the editor(s). MDPI and/or the editor(s) disclaim responsibility for any injury to people or property resulting from any ideas, methods, instructions or products referred to in the content.